ISSN 2394-3777 (Print)
ISSN 2394-3785 (Online)
Available online at www.ijartet.com

International Journal of Advanced Research Trends in Engineering and Technology (IJARTET)
Vol. 5, Special Issue 3, January 2018

DESIGN AND ANALYSIS OF MAIN ROTOR BLADES OF A UTILITY HELICOPTER DURING HOVERING

SHAHID AMEEN KHAN
7th semester, Dept. of Aeronautical Engineering,
S. J. C. Institute of Technology,
Chickballapur, India.
shahidameen07@gmail.com

VIGNESWARAN C M
Assistant Prof., Dept. of Aeronautical Engineering,
S. J. C. Institute of Technology,
Chickballapur, India.
cmvigneswaranaero@gmail.com

ABSTRACT

This paper presents an effective way of reducing the aerodynamic drag of a utility helicopter during hovering. The purpose is to improve the aerodynamic efficiency during hovering by considering the aerodynamic parameters like geometric blade twist, taper ratio, and the airfoil sections at blade root and tip. This paper emphasizes to reduce the rotor tip vortex at the rotor tip by introducing holes at the tip of the blade. The geometry of main rotor blade is generated by using CATIA V5, and the results are analyzed by using Computational Fluid Dynamics (CFD) modeling in STAR CCM+. Performance of the rotor blades with holes and conventional rotor bladesare compared and demonstrated to highlight the effectiveness of the proposed work.

Keywords—*Hovering performance; rotor blade design; rotor tip vortex.*

NOMENCLATURE

C_L – Coefficient of lift
C_D – Coefficient of drag
M – Mach number
M_{DD} -Drag divergence Mach number
L/D – Lift to drag ratio
C_m – Moment coefficient

I. INTRODUCTION

Hovering is one of the most challenging part of flying a helicopter. To hover a helicopter, the pilot must keep the helicopter motionless over a reference point at a constant altitude. To achieve so, the pilot is required to give constant inputs and corrections to counteract the deviation of the helicopter because of the action of its own gusty air striking against the fuselage and flight control surfaces. The ability of the helicopter to hover comes from both the lift component, which is the aerodynamic force developed by the main rotors to overcome the force of gravity and the weight of the aircraft; and the thrust component which acts horizontally to accelerate or decelerate the helicopter in the desired direction. Therefore, during hovering, the lift force, drag force, thrust force, and the weight, are in balance, keeping the helicopter stationary.

A conventional helicopter has three flight control inputs- the cyclic stick, the collective lever, and the anti-torque pedals. The cyclic is used to eliminate the drift in the horizontal plane by controlling the forward, backward, and lateral movement of the helicopter. The collective is used to change the pitch angle of all the main rotor blades, thereby increasing or decreasing the lift derived from the main rotor, giving control of ascent or descent. The pedals are used to control the direction heading by altering the pitch of the tail rotor, thereby increasing or decreasing the tail rotor thrust.

ISSN 2394-3777 (Print)
ISSN 2394-3785 (Online)
Available online at www.ijartet.com

International Journal of Advanced Research Trends in Engineering and Technology (IJARTET)
Vol. 5, Special Issue 3, January 2018

One of the important objective in rotor blade design is to achieve maximum possible aerodynamic performance. The design parameters include the selection of airfoil, blade twist and taper ratio, point of taper initiation, blade root cut out, sweep, point of sweep initiation, and blade tip speed.

The earlier design of rotor blades was mostly symmetrical. NACA 0012 was the classic choice for the design of the helicopter blade sections for many years. Over the time, higher lift to drag ratio was the most demanding characteristic from the airfoil, which lead to the evolution of non-symmetrical versions. Also, high C_L, high $M_{DD,}$ and low C_m are the desired characteristics. However, more lift is required at the root section of the blade rather than at the tip; the tip part sweeps at a higher velocity than the root part, which might entertain transonic flow at the tip of the rotor blade; the tip portion is subjected to vortex effects, which results in undesirable noise. So, each section has its unique requirements and a single airfoil cannot fulfill all the needs. So, a set of varying airfoils are used in the design of the blade section. Blade twist is provided to have a higher angle of attack at the root, so as to provide greater lift. The blade taper is advantageous in having a larger surface area at the root. Both blade twist and taper help to achieve evenly spaced lift distribution along the span of the blade. The cut out at the root of the blade is provided to reduce the effect of potential reverse flow on the retreating blade while the helicopter is flying at higher speeds. It also contributes in nullifying the downwash created at the root of the blade.

Several research works have been established which focused on minimising the hover horsepower while assuring satisfactory forward flight performance [Reference-1]. The numerical optimization method for designing helicopter rotor blades using a coupled free wake-CFD and adjoint method is carried out in [Ref-2]. This method uses Euler flow solver, and adjoint equations are formulated in a rotor coordinate system to perform CFD calculations. The advantage of this method is that satisfactory results can be achieved by minimum computational efforts, especially for a grid generation problem. The sequential quadratic programming (SQP) method is employed to alleviate the dynamic stall effects in helicopter rotor is carried in [Ref-3]. In this method, the geometry of the airfoil is parameterized by the class shape transformation (CST), and the C-topology body-fitted mesh is generated around the airfoil by solving the Poisson equations. Reynolds averaged Navier Stokes (RANS) equations and Lower-Upper Symmetric Gauss-Seidel (LU-SGS) are considered into account for temporal discretization. [2] proposed a system, this fully automatic vehicle is equipped by micro controller, motor driving mechanism and battery. The power stored in the battery is used to drive the DC motor that causes the movement to AGV. The speed of rotation of DC motor i.e., velocity of AGV is controlled by the microprocessor controller.This is an era of automation where it is broadly defined as replacement of manual effort by mechanical power in all degrees of automation. The operation remains an essential part of the system although with changing demands on physical input as the degree of mechanization is increased.

This paper focuses on reducing the high power requirements by reducing the rotor tip vortex for a rotor in hovering condition. The paper is organized as follows:

- The air flow and aerodynamic response during hovering is briefed in the Section- 'Hovering Flight'
- The major complications occurring during hover performance is presented in the Section- 'Problem Formulations'.
- The Section- 'Design Process' provides the methodology for rotor blade design and analyzing using CFD.
- The solutions and converging graphs are depicted in the later sections.

Finally, the section- 'Conclusions' concludes the work presented in this paper.

II. HOVERING FLIGHT

Hovering is the state where the helicopter remains motionless at a reference point, usually a few meters above the ground. To achieve so, the pilot must first cease the directional control (cyclic) until the helicopter has no forward or rearward motion. Then the pilot observes the change in attitude or altitude of the helicopter and makes corrections accordingly by using the collective control to make the helicopter stationary about the reference point.

A. Airflow during hovering

When the blades rotate, the air swirls at the tip of each blade because of the difference in the pressure between the upper and lower surface. This rotor tip vortex from the preceding blade affects the aerodynamic performance of the following blades. Suppose the vortex made by the passing blade lasts for 2 seconds, then the blade rotating about 300 RPM create 600 long-lasting vortex patterns per minute. This continuous generation of the vortex from each blade reduces the effectiveness of the rotor blade.

ISSN 2394-3777 (Print)
ISSN 2394-3785 (Online)
Available online at www.ijartet.com

International Journal of Advanced Research Trends in Engineering and Technology (IJARTET)
Vol. 5, Special Issue 3, January 2018

During hovering, the rotor blades push in a large mass of air downwards with high velocities. The accelerated air below the rotor may reach the speeds up to 100 knots, or maybe more, depending on the gross weight of the helicopter and the size of the rotor. Also, there is a change in effective angle of attack because of downwash, which results in the reduction of lift. To compensate the reduction in this aerodynamic force, the pilot is required to increase the collective pitch to increase the lift and endorse the hover.

Thus, the vortex patterns and change in collective pitch because of downwash increases the induced drag, which demands high power.

B. Ground effect

When the helicopter is operated near the ground or at a height of half of its rotor diameter, there is a significant increase in lift and reduction in drag because of the interference of the solid surface with the airflow pattern. This is called ground effect. In this proximity, the ground interrupts the formation of the rotor tip vortex, thereby reducing the induced drag which results in an increase in lift.

The blade in ground effect operates at a higher angle of attack, which is responsible for more production of lift and increased efficiency because of reduction in induced velocity. If the helicopter is operating beyond the ground effect proximity, there will be an increase in induced velocity, which reduces the effective angle of attack, making the rotor tip vortex interact with the airflow, resulting in the increase of drag, and making the operation of the rotor less efficient.

Therefore, because of increase in efficiency of the rotor system, the pilot reduces the blade pitch angle required to keep the helicopter in hover while in ground effect. Thus, less power is required for the helicopter to hover in ground effect.

C. Vortex ring state

The helicopter descending into its own downwash, resulting in a severe loss of lift and control of the helicopter is known as vortex ring state. It is also called as 'settling with power'. This arises when the helicopter is descending with the higher descent rate, and when the airspeed is less than the Effective Translational Lift (ETL).

When the helicopter descends faster, there will be up-flow at the mast and blade grip area. As this up-flow increases, the blade begins to stall near the hub. This stalling give rise to the formation of the second set of vortices from the center of the rotor system. These vortices reduce the amount of lift produced and increases the descending rate. At this state, the helicopter is said to be operating in its own downwash.

A helicopter encounters this condition when it is attempting to steep power approach while airspeed is near zero, or while attempting to hover out of ground effect without precise attitude control, or when it is attempting hover above hovering ceiling.

III. PROBLEM FORMULATIONS

From the stated data, the following remarks can be made:

- The rotor wake effect is more during hovering.
- The rotor tip vortex reduces the aerodynamic efficiency of the outer rotor blade portions.
- The continuous formation of vortices demands high power requirements during hovering.
- The aerodynamic efficiency of the rotor system increases when the helicopter is in ground effect.
- The helicopter may settle with power and lose its control when it engulfs into its own downwash.
- The rotor tip vertices reduce the effective diameter of the rotor blade, thereby reducing the lift and increasing the drag.

IV. DESIGN PROCESS

The main rotor blade is designed by considering the aerodynamic parameters like- geometric blade twist, taper ratio, and the airfoil sections at blade root and tip. Few holes are made at the tip of the blades and the vortex effect is studied at different conditions.

A. Airfoil selection

The desired characteristics from the airfoil are high C_L, high $M_{DD,}$ and low C_m. Also, each section of the blade will be subjected to different air flow conditions, and each section has its own requirements. So, a single

ISSN 2394-3777 (Print)
ISSN 2394-3785 (Online)
Available online at www.ijartet.com

International Journal of Advanced Research Trends in Engineering and Technology (IJARTET)
Vol. 5, Special Issue 3, January 2018

type of airfoil cannot fulfill all the requirements. Thus, different set of airfoils are used in the design on rotor blade.

For simplification, the root airfoil is taken to be NACA 2412, and tip airfoil is taken as NACA 2408. Both the chosen airfoils are cambered. The advantages of using the using the cambered airfoils are- they have high lift to drag ratio, they have better stall characteristics when compared to symmetrical ones, and they have positive lift at zero and negative angles of attack. The former airfoil has high C_L, which is helpful in producing more lift at the root part. The latter airfoil is chosen as it has high drag divergence mach number.

Figure 1: NACA 2412 airfoil

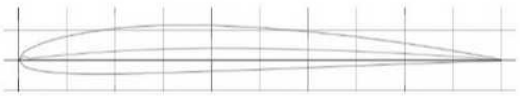

Figure 2: NACA 2408 airfoil

Table 1: **NACA 2412 Airfoil details**

Parameters	**Dimensions**
Thickness	12%
Camber	2%
Trailing edge angle	0%
Lower flatness	70.3%
Leading edge radius	3.2%
Max C_L angle	-6.5º
Max L/D	20917.2
Max L/D angle	-7.5º
Stall angle	-6.5º
Max C_L	78.881
Zero lift angle	-9.0º

Table 2: **NACA 2408 Airfoil details**

Parameters	**Dimensions**
Thickness	8%
Camber	2%
Trailing edge angle	11%
Lower flatness	93%
Leading edge radius	2.6%
Max C_L angle	13.5º
Max L/D	41.453
Max L/D angle	2.5º
Stall angle	2.5º
Max C_L	0.953
Zero lift angle	-2.0º

B. Blade planform

The blade planform can have an important effect on the lift distribution. The rectangular planform increases the lift coefficient, but it also increases the formation of tip vortices. The elliptical planform also increases the coefficient of lift, but it reduces the rotor tip vortices.

C. Blade twist

Blade twist is provided to compensate for unequal lift distribution over the span of the blade and to maintain constant autorotation. Also, for the rotors with the same disc loading, the figure of merit is high for greater twist angle than for the rotor having moderate twist angle.

Thus, the optimum blade twist angle for the hovering performance is between -8º to -15º.

D. Rotor diameter

The diameter of the has a direct impact on the disc loading, induced velocity, and power requirements. The greater the diameter, greater will be the thrust produced and lesser will the disc loading. Also, larger rotor reduces the average induced velocity and lowers the induced power requirement.

The blade geometry is developed by using the designing software- CATIA V5R21. The geometrical data is depicted in the tables 3 and 4.

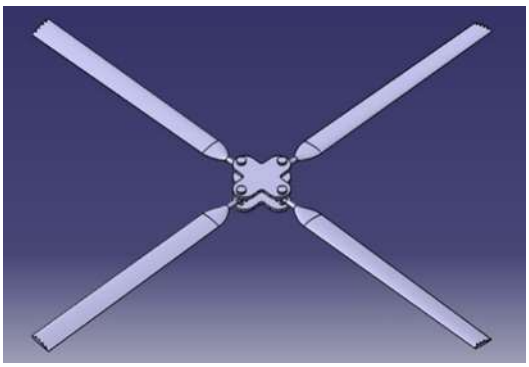

ISSN 2394-3777 (Print)
ISSN 2394-3785 (Online)
Available online at www.ijartet.com

International Journal of Advanced Research Trends in Engineering and Technology (IJARTET)
Vol. 5, Special Issue 3, January 2018

Figure 3: Rotor blade with holes at the tip

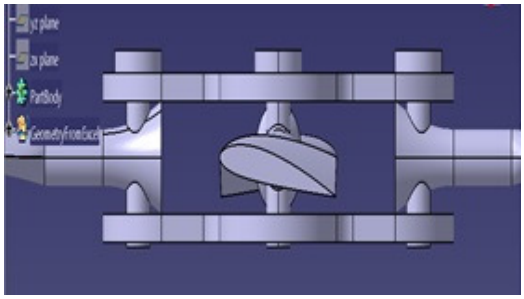

Figure 4: Front view of the rotor blade with twist

V. CFD METHODOLOGY

The designed model of the rotor is imported in the CFD analyzer- Star CCM+. The process of performing the simulation in the CFD divided into three phases. In the first phase, the geometry is imported. Then a region of interest is defined in the geometry, and region of fluid flow is created around the imported geometry. Then the whole domain is meshed. The steps in the second phase is carried by the solver. In this phase, the partial differential equation is integrated over the whole control volume in the region of interest. The differential equations are derived by using the governing laws (Law of conservation of mass, the law of conservation of momentum, and the law of conservation of energy) in each control volume. The partial differential equations are then converted to a system of algebraic equations by generating a set of approximations for the terms in integral equations. Then, these algebraic equations are solved iteratively. An iterative approach is employed because of the non-linear nature of the equations. The iterations are carried until the solution is converged. The closeness of the final solution to the exact solution mainly depends on the size of the mesh and control volumes. Finally, in the third phase, the solution is visualized in the post-processor.

The results are analyzed by comparing the data obtained from the rotor with holes at the tip, with the rotor without holes, at different conditions.

Table 3: **Blade geometry for twist angle of -8º**

Parameters	Dimensions
Root chord	0.5 m
Tip chord	0.5 m
Twist angle	-8º
Taper ratio	1
Rotor span	6.5 m
Rotor diameter	13 m
Hole diameter at rotor tip	0.02 m
Aspect ratio	0.318

Table 4: **Blade geometry for twist angle of -10º**

Parameters	Dimensions
Root chord	0.5 m
Tip chord	0.3 m
Twist angle	-10º
Taper ratio	0.66
Rotor span	7 m
Rotor diameter	14 m
Hole diameter at rotor tip	0.02 m
Aspect ratio	0.318

ISSN 2394-3777 (Print)
ISSN 2394-3785 (Online)
Available online at www.ijartet.com

International Journal of Advanced Research Trends in Engineering and Technology (IJARTET)
Vol. 5, Special Issue 3, January 2018

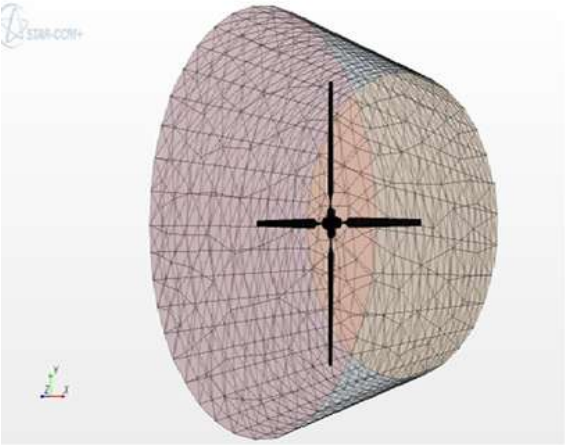

Figure 5: Volume mesh of the rotor

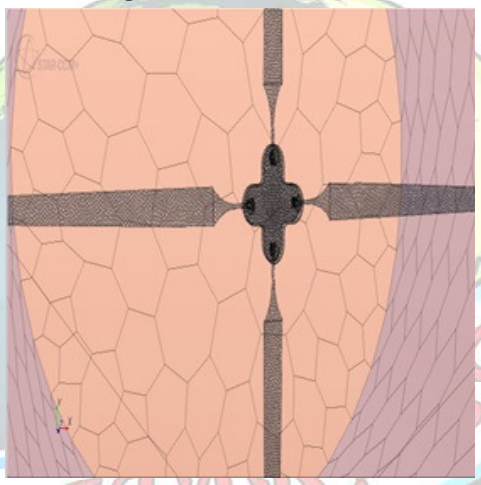

Figure 6: Mesh of the rotor blade

A. **Boundary conditions**

The following boundary conditions are applied for the volume domain.

Table 5: **Boundary conditions**

Air velocity		84 m/s
Rotor speed		300 rpm
At sea level	Pressure	101.325 kPa
	Density	1.125 kg/m^3
At 1000 feet altitude	Pressure	97.97 kPa
	Density	0.997 kg/m^3

The flow is assumed to be steady and coupled, having a constant density throughout the domain. The same boundary conditions are used to carry out the analysis for the rotor with holes at the tip and the rotor without holes.

ISSN 2394-3777 (Print)
ISSN 2394-3785 (Online)
Available online at www.ijartet.com

International Journal of Advanced Research Trends in Engineering and Technology (IJARTET)
Vol. 5, Special Issue 3, January 2018

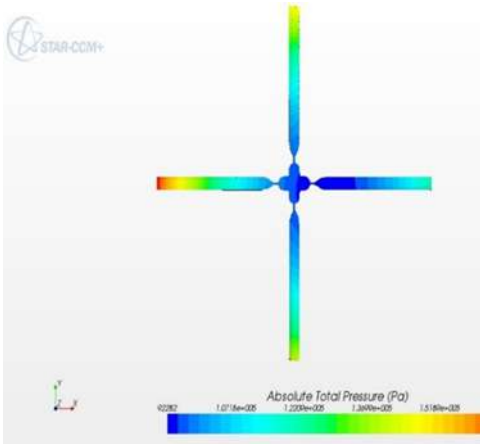

Figure 7: Scalar result for the rotor blade (-10º twist angle) with holes at sea level

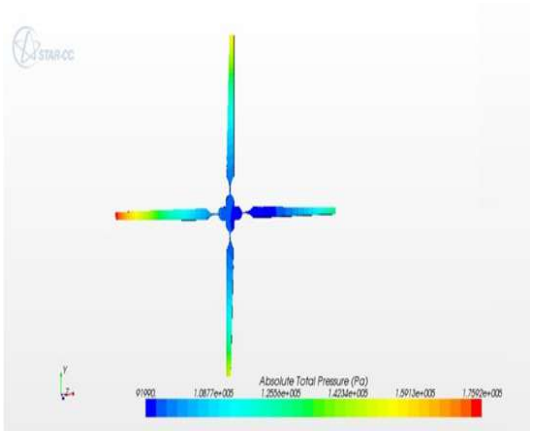

Figure 8: Scalar result of the rotor blade (-10º twist angle) without holes at sea level

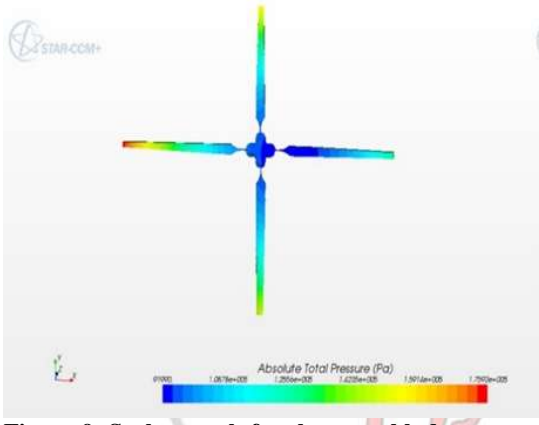

Figure 9: Scalar result for the rotor blade (-10º twist angle) with holes at 1000 feet

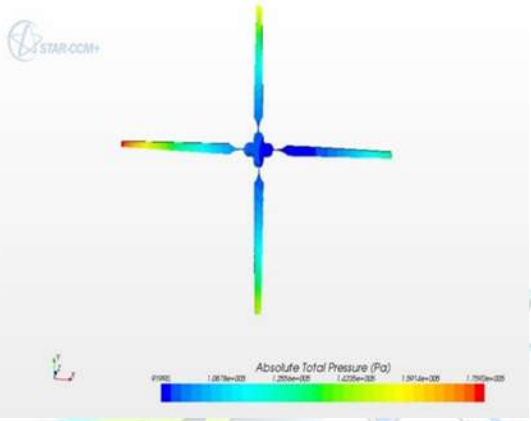

Figure 10: Scalar result for the rotor blade (-10º twist angle) without holes at 1000 feet

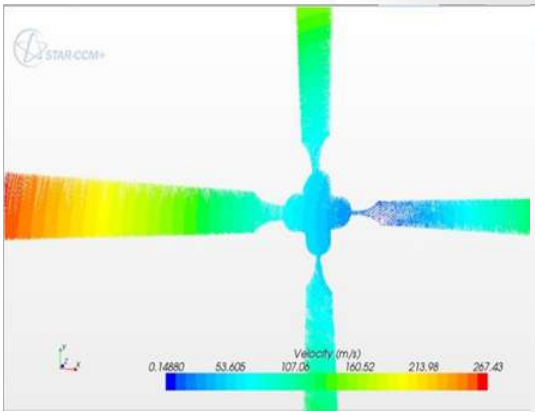

Figure 11: Vector result for the rotor blade (-10º twist angle) with holes at sea level

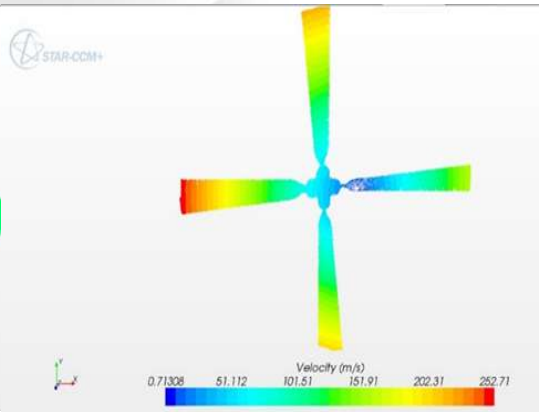

Figure 12: Vector result for the rotor blade (-10º twist angle) without holes at sea*level*

ISSN 2394-3777 (Print)
ISSN 2394-3785 (Online)
Available online at www.ijartet.com

International Journal of Advanced Research Trends in Engineering and Technology (IJARTET)
Vol. 5, Special Issue 3, January 2018

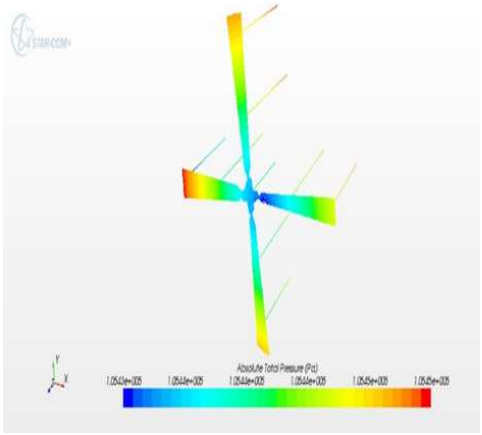

Figure 13: Flow pattern for the rotor blade (-10º twist angle) with hole at sea level

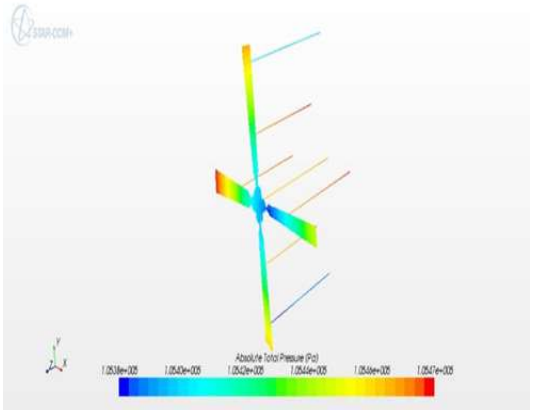

Figure 14: Flow pattern for the rotor blade (-10º twist angle) without hole at sea level

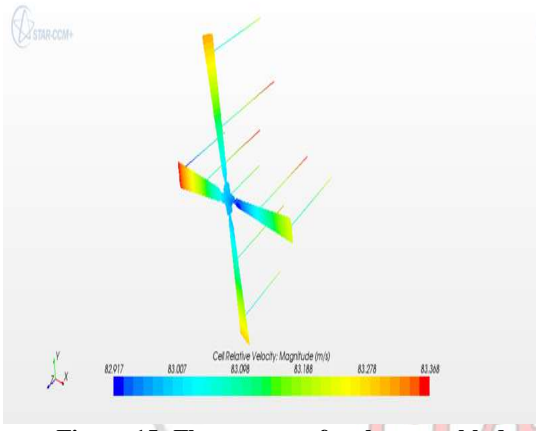

Figure 15: Flow pattern for the rotor blade (-10º twist angle) with hole at 1000 feet

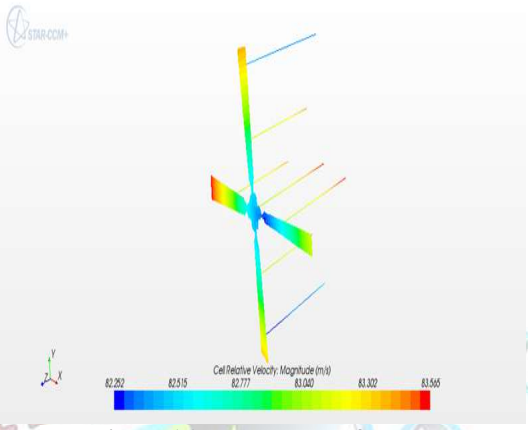

Figure 16: Flow pattern for the rotor blade (-10º twist angle) without hole at 1000 feet

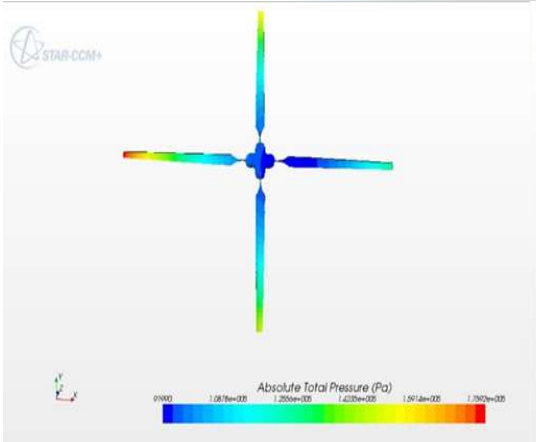

Figure 17: Scalar result for the rotor blade (-8º twist angle) with holes at sea level

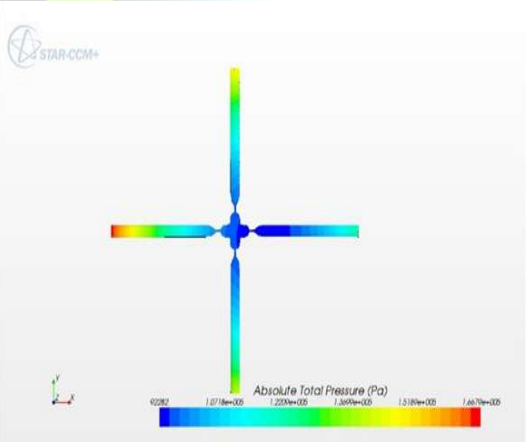

Figure 18: Scalar result for the rotor blade (-8º twist angle) without holes at sea level

ISSN 2394-3777 (Print)
ISSN 2394-3785 (Online)
Available online at www.ijartet.com

International Journal of Advanced Research Trends in Engineering and Technology (IJARTET)
Vol. 5, Special Issue 3, January 2018

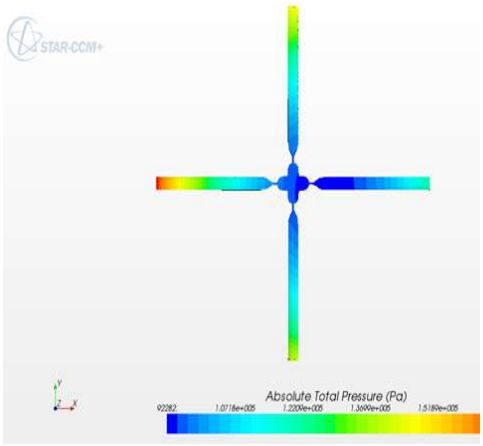

Figure 19: Scalar result for the rotor blade (-8º twist angle) with holes at 1000 feet

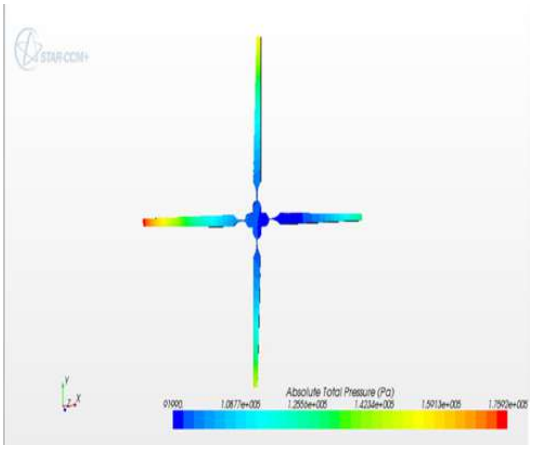

Figure 20: Scalar result for the rotor blade (-8º twist angle) without holes at 1000 feet

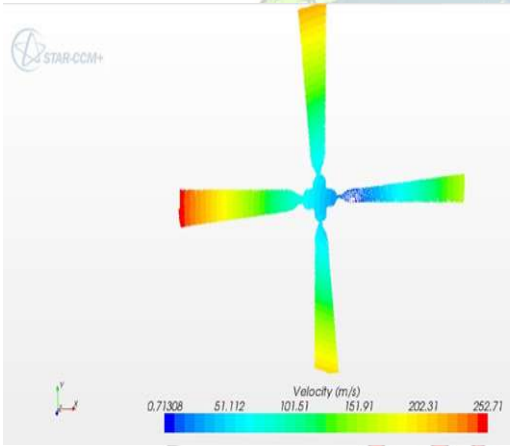

Figure 21: Vector result for the rotor blade (-8º twist angle) without holes at sea level

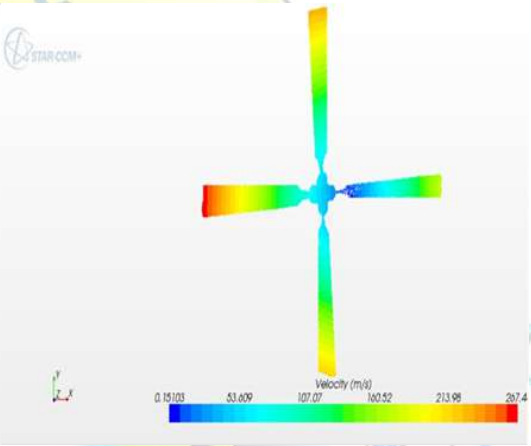

Figure 22: Vector result for the rotor blade (-8º twist angle) with holes at 1000 feet

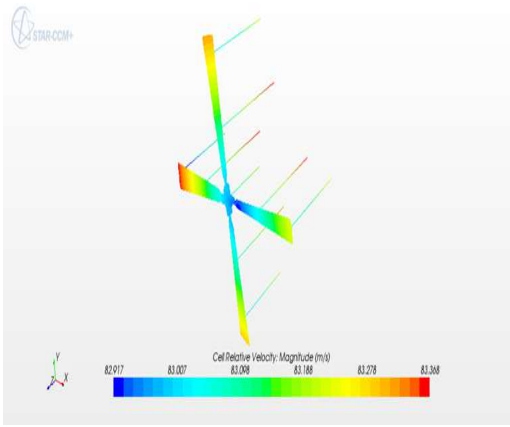

Figure 23: Flow pattern for the rotor blade (-8º twist angle) with hole at sea level

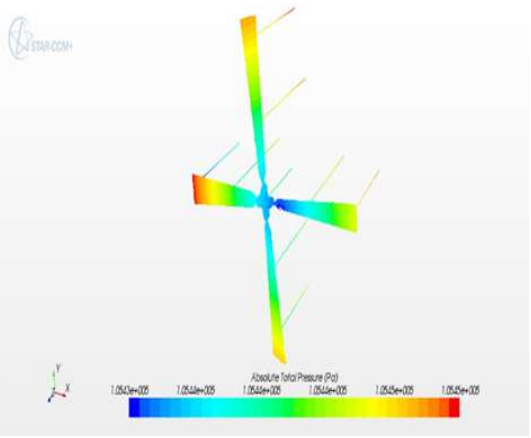

Figure 24: Flow pattern for the rotor blade (-8º twist angle) without hole at sea level

ISSN 2394-3777 (Print)
ISSN 2394-3785 (Online)
Available online at www.ijartet.com

International Journal of Advanced Research Trends in Engineering and Technology (IJARTET)
Vol. 5, Special Issue 3, January 2018

VI. RESULTS

The results are calculated by several iterations until the converging value is obtained, i.e., until the exact solution and obtained solution is approximately equal and repetitive.

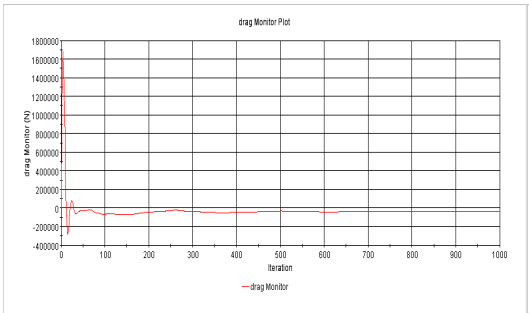

Figure 25: Drag value convergent graph for the rotor blade (-10º twist angle) at sea level

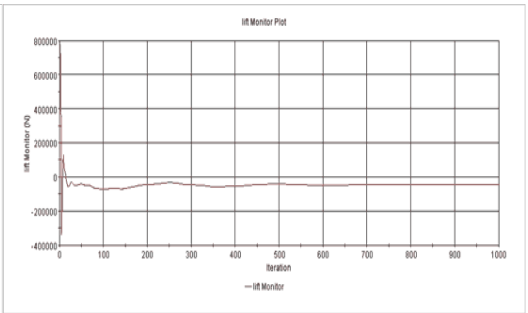

Figure 26: Lift value convergent graph for the rotor blade (-10º twist angle) at sea level

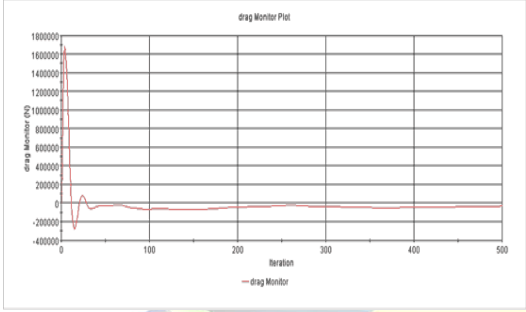

Figure 31: Drag value convergent graph for the rotor blade (-10º twist angle) at 1000 feet

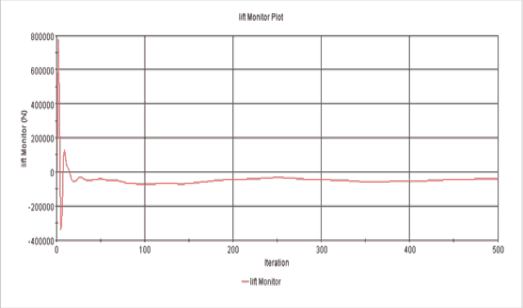

Figure 32: Lift value convergent graph for the rotor blade (-10º twist angle) at 1000 feet

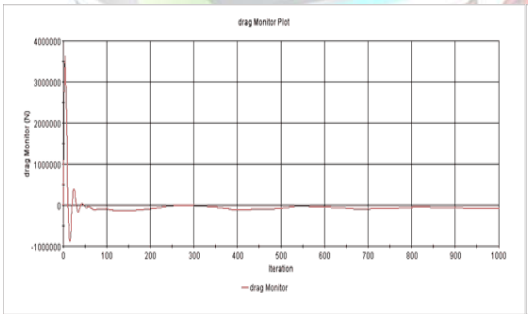

Figure 33: Drag value convergent graph for the rotor blade (-8º twist angle) at sea level

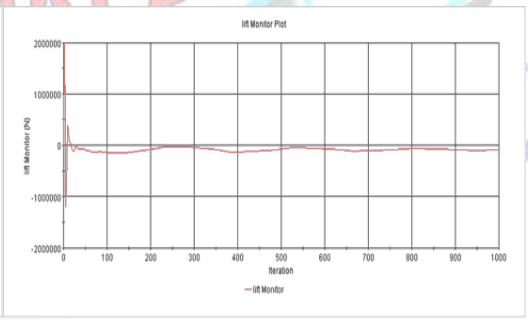

Figure 34: Lift value convergent graph forthe rotor blade (-8º twist angle) at sea level

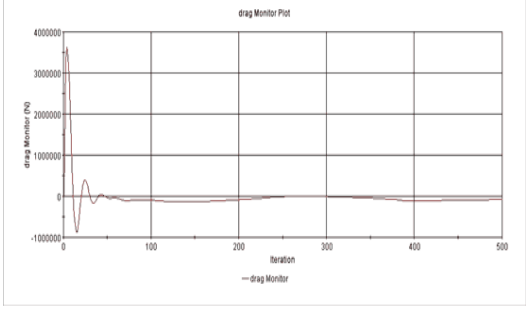

Figure 35: Drag value convergent graph for the

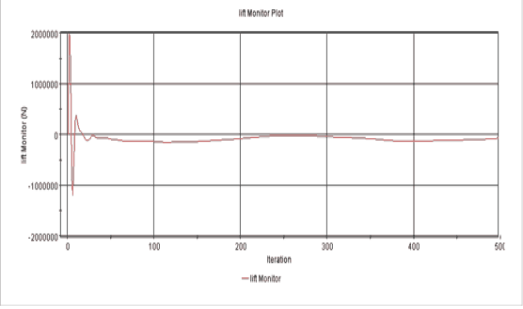

Figure 36: Lift value convergent graph for the

ISSN 2394-3777 (Print)
ISSN 2394-3785 (Online)
Available online at www.ijartet.com

International Journal of Advanced Research Trends in Engineering and Technology (IJARTET)
Vol. 5, Special Issue 3, January 2018

rotor blade (-8º twist angle) at 1000 feet **blade (-8º twist angle) at 1000 feet**

Table 6: **RESULTS DATA**

Twist angle	Condition		Lift (N)	Drag (N)	L/D
-8º	With holes	Sea level	699.3559	582.6768	1.200246689
		1000 feet	699.473937	582.7539	1.200279810
	Without holes	Sea level	698.66667	584.6102	1.19509820
		1000 feet	698.68786	584.6572	1.19503827
-10º	With holes	Sea level	515.81457	432.52505	1.1925657
		1000 feet	515.89691	432.52593	1.1927536
	Without holes	Sea level	516.1336	433.8000	1.18979621
		1000 feet	516.30126	434.02032	1.18957855

VI. CONCLUSIONS

The design of rotor blade with holes at the tip and an attempt to reduce the aerodynamic drag because of rotor tip vortex is presented in this paper. The model is created in CATIA V5R21, and analysis is done by using CFD software- Star CCM+. The rotor blades with holes at the tip are tested at sea level and at an altitude of 1000 feet, and its performance is compared with the conventional rotor blade (without holes at the tip).
For a rotor at hovering condition, it is observed that:

- There is a slight decrease in drag for the rotor blade for twist angle of -8º with holes the tip when compared to that of the conventional rotor blade.
- The lift to drag ratio for the rotor blade for twist angle of -8º is greater than that of the conventional rotor blade.
- There is a slight decrease in drag for the rotor blade for twist angle of -10º with holes the tip when compared to that of the conventional rotor blade.
- The lift to drag ratio for the rotor blade for twist angle of -10º is greater than that of the conventional rotor blade.

The studies can be made for the effect of holes for a helicopter in forward flight, and other maneuvering flight conditions. The structural and vibrational study can also be done for the designed rotor. More studies can be made on the effective diameter of the holes and their position on the rotor blade.

REFERENCES

[1] Joanne L. Walsh, Gene J. Bingham, and Michael F Riley, 'Optimization methods applied to the aerodynamic design of helicopter rotor blades', NASA Technical Memorandum, 1987.

[2] Christo Ananth, M.A.Fathima, M.Gnana Soundarya, M.L.Jothi Alphonsa Sundari, B.Gayathri, Praghash.K, "Fully Automatic Vehicle for Multipurpose Applications", International Journal Of Advanced Research in Biology, Engineering, Science and Technology (IJARBEST), Volume 1,Special Issue 2 - November 2015, pp.8-12.

[3] H. Farrokhfall, A. R. Pishwar, 'Aerodynamic shape optimization of hovering rotor blades using a coupled free wake-CFD and adjoint method', Aerospace Science and Technology, Volume 28, July 2013.

[4] Ngoc Anh Vu, Jae Woo Lee, and Jung Il Shu, 'Aerodynamic design optimization of helicopter blades including airfoil shape for hover performance', Chinese Journal of Aeronautics, February 2013.
Rado and H. Suhl, Eds. New York: Academic, 1963, pp. 271-350.

[5] Wang Qing, Zhao Qijun, and Wu Qi, 'Aerodynamic shape optimization for alleviating dynamic stall characteristics of helicopter rotor airfoil', Chinese Journal of Aeronautics, April 2015.

[6] J. Gordon Leishman, 'Principles of Helicopter Aerodynamics